On velocity observers for a planar robot subject to non-smooth impacts

Sergio Galeani, Laura Menini, Antonio Tornambè

Abstract— **The goal of this paper is to compare the performances of two different velocity observers, a full order one and a reduced order one, when used to estimate the velocity vector of a planar robot subject to impacts with the environment, modelled as perfectly rigid. Both the sensitivity of the observers to quantization errors in the position measurements and their behaviour in closed-loop are investigated.**

Keywords— **Mechanical systems, non-smooth impacts, velocity observers.**

I. Introduction

THE problem of modeling mechanical systems subject to non-smooth impacts is far from being solved in its generality, especially when multiple impacts or the effects of friction have to be taken into account [1]. Nevertheless, several authors have studied mechanical systems subject to impacts from the control point of view: typical applications are free-flying space robots [2], [3] and robotic systems where the impacts between the robot and the environment constitute a significant feature of the robot task [4], [5]. The problem of modeling and controlling a one-degree-of-freedom impact between two bodies subject to elastic/plastic deformations is considered in [6]. In [7], a new sensor-referenced control method using positive acceleration feedback together with a switching control strategy is developed for robot impact control and force regulation. The problem of modeling and controlling the impact between the end-effectors of two multi-DOF (Degree-Of-Freedom) cooperating manipulators is considered in [8].

Recently, the control of finite-dimensional mechanical systems with unilateral constraints has been studied, with the aim of developing a general theory, in [9] and in [10]. In this last paper, a Liapunov analysis of PD-like control laws for mechanical systems subject to impacts can be found. In particular, when impacts are modelled as non-smooth the overall mechanical system exhibits a hybrid behaviour, *i.e.*, its evolution is governed by a continuous time dynamics between each pair of consecutive impact times, whereas at impact times the state undergoes sudden finite jumps.

The need for velocity observers in the control of mechanical systems and, in particular, of robots, is widely recognized [11]-[14]. As a matter of fact, velocity measurements are often affected by noise, which severely limits the performance achievable by control laws making use of such measurements. In [11], non-linear observers have been designed by means of differential-geometry-based techniques for robots having elastic joints. In [12], an observer is designed for rigid robots, and its use for point to point control and for trajectory control is illustrated. In [13], both "smooth" observers and "sliding" observers are used for tracking control. In [14], observer-based control laws are derived by means of a passivity approach, achieving a linear output-feedback controller also used for tracking purposes.

S. Galeani, L. Menini and A. Tornambè are with Dipartimento di Informatica, Sistemi e Produzione – Università di Roma Tor Vergata – Via del Politecnico, 1 – 00133 Roma, Italy. E-mail: [galeani,menini,tornambe]@disp.uniroma2.it .

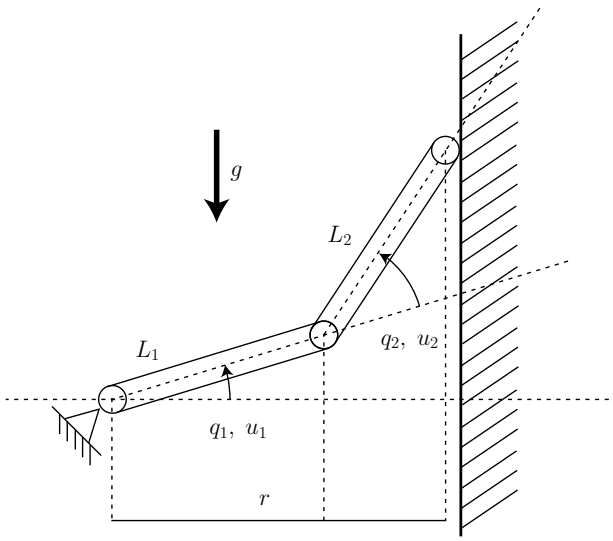

Fig. 1. Two-DOF planar robot arm

In this paper, two different hybrid velocity observers, taking into account the presence of the impacts by suitable switches at the impact times, are considered. The first is a full order observer, whose continuous-time design is based on the linearization of the model of the robot around a given equilibrium point (as in [16], [18]), whereas the second is a reduced order observer, proposed in [17].

The performances of the two observers are compared, both in open-loop and in closed-loop (*i.e.*, when a PD control law making use of their estimates is used to stabilize a contact configuration for the robot), exploring, in particular, their robustness versus quantization errors in the position measurements.

II. Description of the mechanical system

Consider the two-DOF planar robot arm depicted in Figure 1. The robot arm is constituted by a base body and two links, which are interconnected by two rotational joints so to form a planar chain. The robot is moved in a vertical plane by the action of two torques $u_1(t)$ and $u_2(t)$ that are exerted by two motors on the two joints. The two links have respective length L_i and mass M_i, $i = 1, 2$, whereas

the two joints have negligible mass and inertia. The joint angles $q_1(t)$ and $q_2(t)$ are taken as the generalized coordinates, which uniquely describe the configuration of the robot arm in the motion plane.

An infinitely rigid and massive surface is perpendicular to the motion plane at a distance r from the joint connecting the base body to the first link of the chain (see Figure 1). Assume that $L_1 < r < L_1 + L_2$, so that the end-effector (which is also assumed to be infinitely rigid) is the only part of the robot arm that can collide with the surface, and contact configurations actually exist.

The distance of the robot end-effector from the infinitely rigid and massive surface is

$$r - L_1 \cos(q_1(t)) - L_2 \cos(q_1(t) + q_2(t)); \tag{1}$$

then, the mechanical system is subject to the inequality constraint $f(q(t)) \leq 0$, where $f(q) := L_1 \cos(q_1) + L_2 \cos(q_1 + q_2) - r$ and $q(t) := \begin{bmatrix} q_1(t) & q_2(t) \end{bmatrix}^T$ is the vector of the generalized coordinates. Let $J(q) := \dfrac{\partial f(q)}{\partial q}$ be the gradient row vector of $f(q)$.

The kinetic energy of the robot arm at time $t \geq t_0$ is $T(q(t), \dot{q}(t)) = \dfrac{1}{2}\, \dot{q}^T(t)\, B(q(t))\, \dot{q}(t)$, where the components of the positive definite generalized inertia matrix $B(q)$ are given by

$$\begin{aligned} B_{1,1}(q) &= \frac{L_1^2 M_1}{3} + \frac{M_2}{6}\left(6L_1^2 + 2L_2^2 + 6L_1 L_2 \cos(q_2)\right), \\ B_{1,2}(q) &= B_{2,1}(q) = \frac{M_2}{6}\left(2L_2^2 + 3L_1 L_2 \cos(q_2)\right), \\ B_{1,2}(q) &= \frac{L_2^2 M_2}{3}. \end{aligned}$$

The potential energy of the robot is given by:

$$U(q) := g\left(L_1\left(\frac{1}{2}\, M_1 + M_2\right)\sin(q_1) + \frac{1}{2}\, L_2\, M_2\, \sin(q_1 + q2)\right).$$

By using the well-known Lagrange equations, for $t \in (t_i,\, t_{i+1})$, the equations of motion of the robot are given by

$$B(q)\, \ddot{q}(t) + C(q(t), \dot{q}(t))\, \dot{q}(t) + h(q(t)) = \tau(t), \tag{2}$$

where $h(q) := \dfrac{\partial U(q)}{\partial q}$ and $C(\cdot, \cdot)$ takes into account centrifugal and Coriolis terms. For later use, equation (2) can be rewritten as

$$\ddot{q}(t) = F(q(t), \dot{q}(t)) + B^{-1}(q(t))\, \tau(t).$$

Let the coefficient of restitution e characterizing the non-smooth impacts be equal to 1 (we recall that $e = 1$ for elastic non-smooth impacts, *i.e.*, when there is no loss of kinetic energy due to the non-smooth impacts). For each impact time t_i, in order to compute the post-impact velocity $\dot{q}(t_i^+)$ as a function of the pre-impact velocity $\dot{q}(t_i^-)$, we use the *kinetic metric approach* [1, Chapter 6]:

$$\dot{q}(t_i^+) \;=\; Z(q(t_i))\, \dot{q}(t_i^-), \quad i \in \mathbb{N}, \tag{3}$$

where

$$Z(q) := I_n - \frac{2}{J(q) B^{-1}(q) J^T(q)}\, B^{-1}(q) J^T(q) J(q). \tag{4}$$

Notice that, as could be expected, $Z(q)$ depends on the system's generalized position q, on the system's parameters (via $B(q)$) and on the constraint (via $J(q)$). More detailed explanations about the physical meaning of (4) can be found in [1].

III. The proposed velocity observers

In this section, we describe the two observers that are under comparison. The observer in Subsection III-A appeared in [18] as a modification of the one proposed in [16] for linearly observable systems: its design is based on the linearization of the continuous-time dynamics of the robot about a suitable equilibrium point $q = q_e$, $\dot{q} = 0$. The reduced order observer described in Subsection III-B was proposed in [17].

A. Full order observer

The full order observer is a dynamic system having $\begin{bmatrix} \hat{q}^T(t) & \hat{v}^T(t) \end{bmatrix}^T \in \mathbb{R}^4$ as state vector, being $\hat{q}(t)$ and $\hat{v}(t)$ the estimates of $q(t)$ and $v(t)$, respectively. Its dynamics are given by:

$$\begin{aligned} \dot{\hat{q}}(t) &= \hat{v}(t) + G_1(q(t) - \hat{q}(t)), \quad t \in (t_i, t_{i+1}), && \text{(5a)} \\ \dot{\hat{v}}(t) &= F(\hat{q}(t), \hat{v}(t)) + B^{-1}(\hat{q}(t))\, \tau(t) + G_2(q(t) - \hat{q}(t)), \\ &\qquad t \in (t_i, t_{i+1}), && \text{(5b)} \\ \hat{q}(t_i^+) &= \hat{q}(t_i^-), \quad i \in \mathbb{N}, && \text{(5c)} \\ \hat{v}(t_i^+) &= Z(\hat{q}(t_i))\hat{v}(t_i^-), \quad i \in \mathbb{N}, && \text{(5d)} \end{aligned}$$

where the matrix $G = \begin{bmatrix} G_1^T & G_2^T \end{bmatrix}^T \in \mathbb{R}^{4\times 2}$ is chosen so that, letting

$$\begin{aligned} A_e &= \left[\begin{array}{cc} 0_{2\times 2} & I_2 \\ \dfrac{\partial F(q,\dot{q})}{\partial q} & \dfrac{\partial F(q,\dot{q})}{\partial \dot{q}} \end{array}\right]\Bigg|_{q=q_e, \dot{q}=0}, \\ C_e &= \begin{bmatrix} I_2 & 0_{2\times 2} \end{bmatrix}, \end{aligned}$$

all the eigenvalues of $A_e - GC_e$ have real part smaller than zero.

B. Reduced order observer

The state of the reduced order observer is a vector $\xi \in \mathbb{R}^2$. The dynamics of the observer are given by:

$$\begin{aligned} \dot{\xi}(t) &= F(q(t), \hat{v}(t)) + B^{-1}(q(t))\, \tau(t) - \alpha\, \xi(t) - \alpha^2\, q(t), \\ &\qquad t \in (t_i, t_{i+1}), && \text{(6a)} \\ \hat{v}(t) &= \xi(t) + \alpha\, q(t), \quad t \in (t_i, t_{i+1}), && \text{(6b)} \\ \xi(t_i^+) &= Z(\hat{q}(t_i))\left(\xi(t_i^-) + \alpha\, q(t)\right) - \alpha\, q(t), \quad i \in \mathbb{N}, && \text{(6c)} \end{aligned}$$

where α is a positive real number (to be chosen suitably high to guarantee faster convergence of the estimation error).

IV. Comparison between the proposed velocity observers

In this section, the two observers proposed above are compared through simulations. The parameters of the robot and the environment have been chosen as follows: $g = 9.808$ m/s^2, $M_1 = 0.5$ kg, $M_2 = 0.4$ kg, $L_1 = 0.25$ m, $L_2 = 0.2$ m, and $R = 0.29$ m. An equilibrium position has been chosen $q_e \approx [1.05 \quad -0.52]^T$ rad, which corresponds to a constant input $\tau_e \approx [1.13 \;\; 0.34]^T$ N m. Such an equilibrium position is not in the admissible region, since $f(q_e) > 0$, but it is quite close to the boundary. Then, by choosing a control law $\tau(t) = \tau_e + k_p\,(q_e - q(t))$, with a suitable value of k_p, significant trajectories (*i.e.*, having a sufficient number of impacts, and remaining in a suitable neighbourhood of the equilibrium position) are obtained.

A. First set of simulations: observers' parameters tuning

It is noticed that, for both observers, the convergence rate of the estimation errors to zero can be tuned. For the full order observer, this is achieved through the choice of the eigenvalues of the matrix $A_e - GC_e$, whereas, for the reduced order observer, it is achieved through the choice of the constant α. Then, in order to be fair in the comparison, some simulations (from different initial conditions in the admissible region, and with different values of the proportional gain k_p) have been carried out in order to choose such parameters so that, under ideal conditions (*i.e.*, when no quantization error is present), the two observers give similar exponential rates of convergence. The values chosen at the end of such a first set of simulations are

$$\sigma(A_e - GC_e) = \{-10,\ -11,\ -12,\ -13\}, \tag{7}$$

and

$$\alpha = 6. \tag{8}$$

Such parameters of the two observers will be kept constant through the rest of the paper. Among the various initial conditions and values of k_p used in this first set of simulations, the values

$$q(0) = \begin{bmatrix} 1.15 \\ -0.49 \end{bmatrix} \text{ rad}, \quad \dot{q}(0) = \begin{bmatrix} 0.5 \\ -0.2 \end{bmatrix} \text{ rad/s}, \tag{9a}$$

$$k_p = 3 \text{ N m}, \tag{9b}$$

were chosen as particularly representative of the typical behaviour of the system. For this reason and for the sake of a clear comparison, they will also be used in the next subsection IV-B. In order to give an idea of the amplitude of the considered motions (it is stressed that the full order observer is designed on the basis of the linearization about an equilibrium position q_e), the postures assumed by the two links during the first six seconds of simulation are reported in Figure 2 with continuous lines, whereas the posture corresponding to q_e is reported with a dashed line, and the rigid boundary of the admissible region is reported with a dotted line. The results of the first six seconds of simulation of the full order observer with the choices (7) and (9) are reported in Figures 3-5. As it can be seen from Figure 5, where the time behaviour of the components of the estimation errors $\tilde{q}(t)$ and $\tilde{v}(t)$ are reported, after one second the estimation errors are negligible. Analogously, the results of the first six seconds of simulation of the reduced order observer with the choices (8) and (9) are reported in Figures 6-7. Notice that the position variables are not reported for this simulation, since there are not related estimates and their time behaviour is exactly the one in Figure 3 (continuous line). As shown in Figure 7, after one second the estimation errors are negligible in this case too (compare with Figure 5).

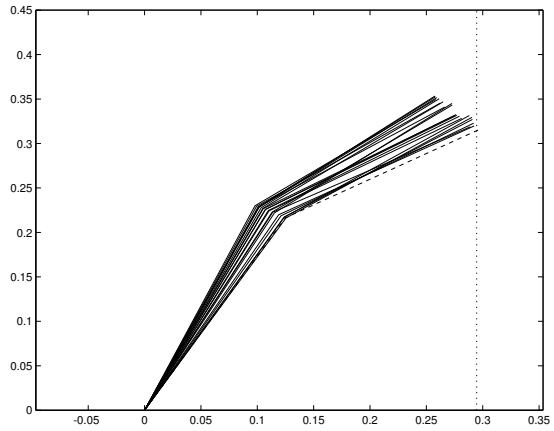

Fig. 2. Postures assumed by the robot during the simulations of the first and second set.

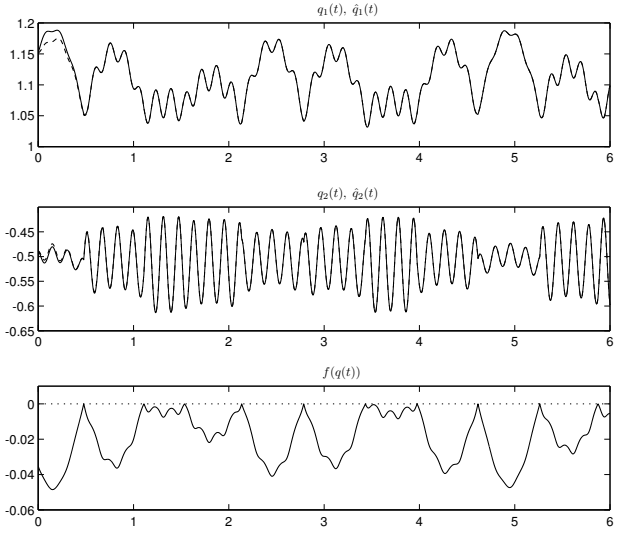

Fig. 3. Time behaviour of the position variables (continuous line) and of their estimates (dashed line) obtained with the full order observer in ideal conditions (no quantization). In the lowest plot the time behaviour of $f(q(t))$ is reported, together with a dotted line indicating the limit value of zero, in order to emphasize the impact times.

B. Second set of simulations: sensitivity to quantization

In this subsection, it is assumed that the position variables are measured through a physical device subject to quantization, *e.g.*, an encoder dividing the $2\,\pi$ angle into N steps, so that, in both observers (5) and (6), the vector $q(t)$

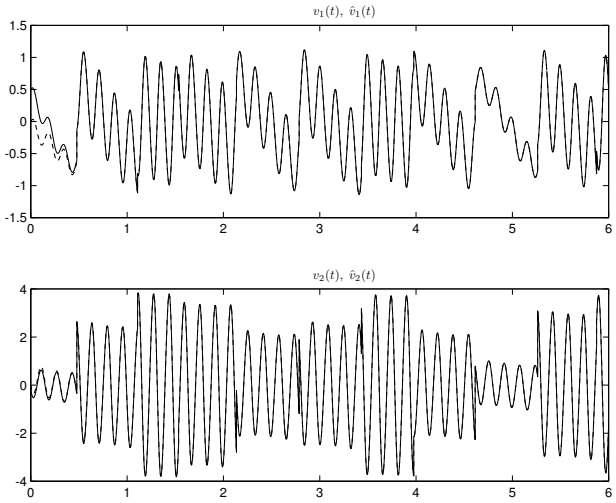

Fig. 4. Time behaviour of the velocity variables (continuous line) and of their estimates (dashed line) obtained with the full order observer in ideal conditions (no quantization).

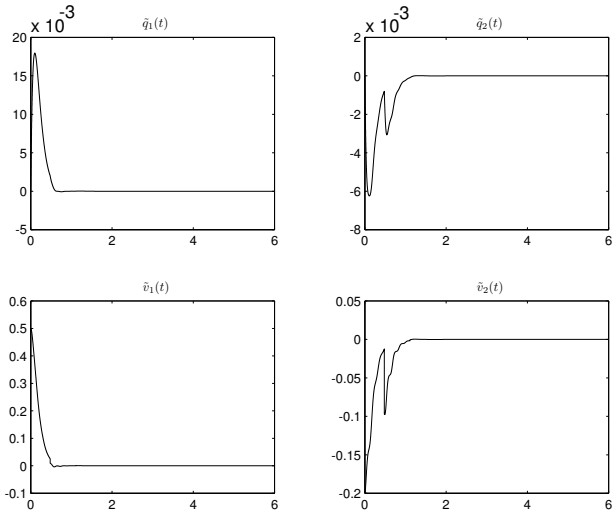

Fig. 5. Time behaviour of the estimation errors obtained with the full order observer in ideal conditions (no quantization).

is replaced by its quantized version $y(t)$. The following values of N have been chosen $N \in \{4096,\ 2048,\ 1024,\ 512\}$, and tested with both observers. In Figure 8, the time behaviour of $\|\tilde{v}(t)\| = \sqrt{\tilde{v}_1^2(t) + \tilde{v}_2^2(t)}$ is reported with dashed lines for the errors deriving from the application of the full order observer with quantized measurement (notice that, for the full order observer, $\tilde{v}(t)$ is not the error vector, which is a four dimensional vector containing also the components of $\tilde{q}(t)$) and with a continuous line for the ideal measurement. In Figure 9, the time behaviour of $\|\tilde{v}(t)\|$ is reported with dashed lines for the errors deriving from the application of the reduced order observer with quantized measurement and with a continuous line for the ideal measurement. By comparing Figures 8 and 9, it is possible to see that the velocity estimates given by the reduced order observer are more sensitive to quantization errors (but this fact is not dramatic).

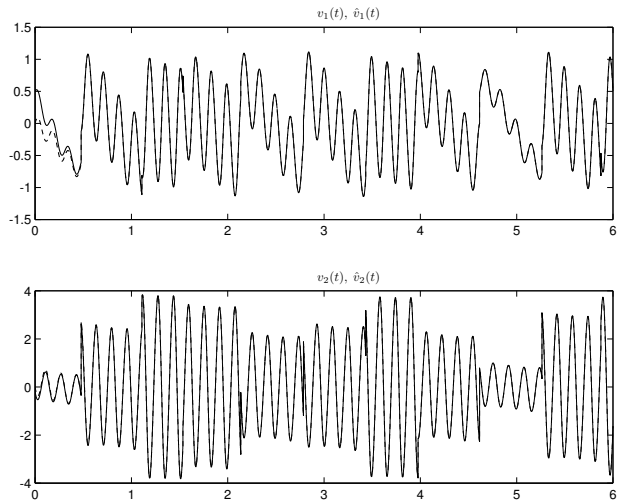

Fig. 6. Time behaviour of the velocity variables (continuous line) and of their estimates (dashed line) obtained with the reduced order observer in ideal conditions (no quantization).

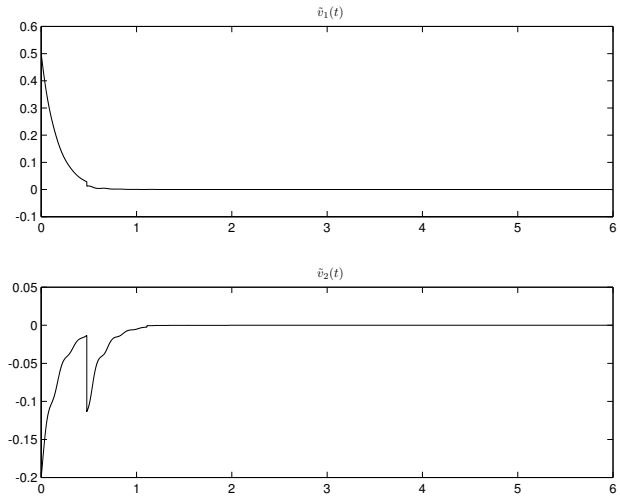

Fig. 7. Time behaviour of the estimation errors obtained with the reduced order observer in ideal conditions (no quantization).

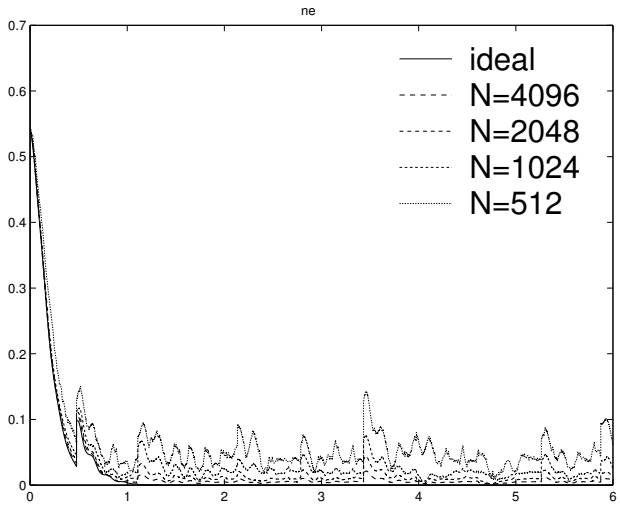

Fig. 8. Time behaviour of $\|\tilde{v}(t)\|$ in the case of ideal (continuous line) and quantized (dashed) measurements for the full order observer.

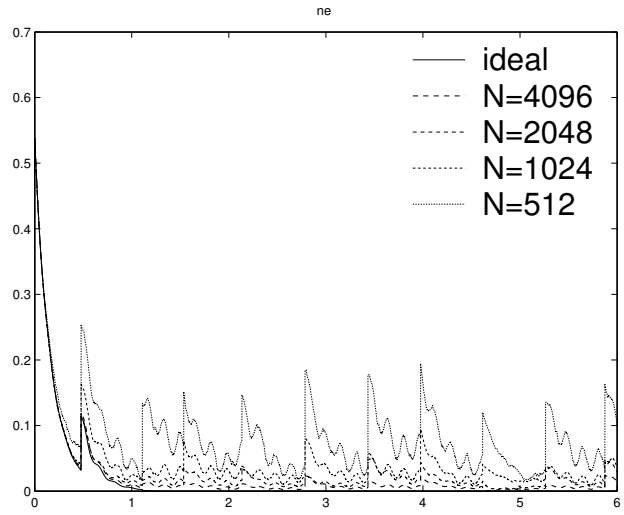

Fig. 9. Time behaviour of $\|\tilde{v}(t)\|$ in the case of ideal (continuous line) and quantized (dashed) measurements for the reduced order observer.

C. Third set of simulations: closed-loop behaviour

In this subsection, the proposed observers have been used for control purposes. In particular, an equilibrium position q_L corresponding to a contact configuration with the environment, *i.e.*, such that $f(q_L) = 0$, has been chosen as $q_L \approx [1.05 \;\; -0.49]^T$ rad, which corresponds to a constant input $\tau_L \approx [1.13 \;\; 0.33]^T$ N m.

A PD control law $\tau(t) = \tau_L + k_p\,(q_L - \hat{q}(t)) - k_v\,\hat{v}(t)$, with $k_p = 3$ N m and $k_v = 0.1\,\sqrt{(3)}$ N s m, has been used, first by using the estimates $\hat{q}(t)$ and $\hat{v}(t)$ obtained with the full order observer, and then by replacing $\hat{q}(t)$ with the measured $q(t)$ and by using the estimate $\hat{v}(t)$ obtained with the reduced order observer. The behaviour of the closed-loop systems obtained (under ideal conditions, *i.e.*, with no quantization errors in the measurements of the position variables) by using the full order observer and the reduced order observer is depicted in Figure 10 and in Figure 11, respectively. The same simulations have been repeated by assuming quantized measurements, with $N = 1024$. The corresponding results are reported in Figures 12 and 13. From the lowest plot in both figures, it is possible to see that the contact condition is satisfactorily reached in both cases. However, by looking at the time behaviour of $q_2(t)$ (such a variable has just small variations, hence its time behaviour emphasizes the problems due to quantization), it is evident that in neither one of the two cases the stabilization of the desired position q_L is obtained, and the undesired oscillations are much more evident when the full order observer is used. This is probably a consequence of the fact that the PD control law is using, in the case of the full order observer, just the estimates of the position variables given by the observer, and not, as in the case of the reduced order observer, the quantized measurements themselves. However, it is worth to notice that the simulation in Figure 12 is practically the worst case between the many others performed with different initial conditions.

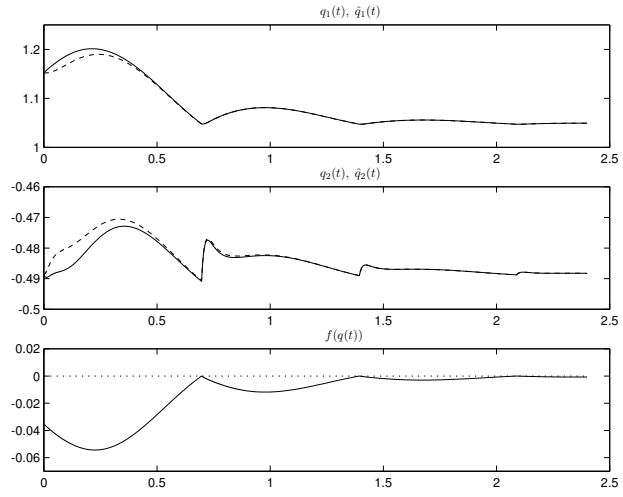

Fig. 10. Time behaviour of the position variables (continuous line) and of their estimates (dashed line) obtained by applying a closed-loop PD control law, making use of the estimates obtained with the full order observer in ideal conditions (no quantization). In the lowest plot the time behaviour of $f(q(t))$ is reported, together with a dotted line indicating the limit zero value, in order to emphasize the impact times.

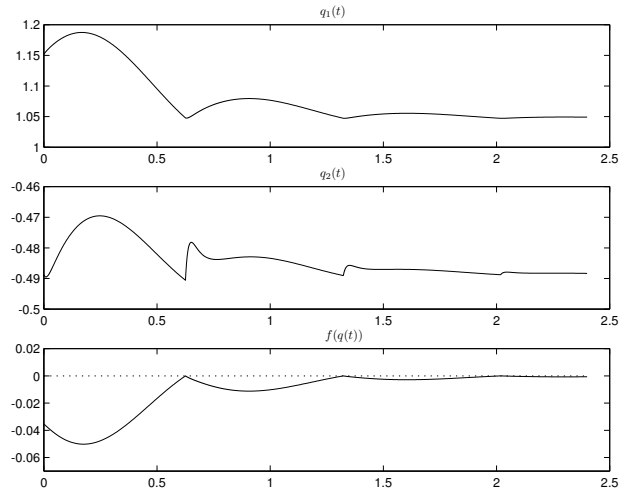

Fig. 11. Time behaviour of the position variables obtained by applying a closed-loop PD control law, making use of the velocity estimates obtained with the reduced order observer in ideal conditions (no quantization). In the lowest plot the time behaviour of $f(q(t))$ is reported, together with a dotted line indicating the limit zero value, in order to emphasize the impact times.

V. Concluding remarks

A simulative comparison between two kinds of velocity observers (already proposed in the literature [17], [18]) for mechanical systems subject to impacts has shown that both kinds of observers are quite robust to quantization errors, also when used for closed-loop control.

While a simple two link robot has been used for the sake of clarity and to make the analysis more readily understandable, the underlying theory in [17], [18] is applicable to more complex systems, and considerations similar to those found in this paper can be drawn when the same observers are used for such more complex systems.

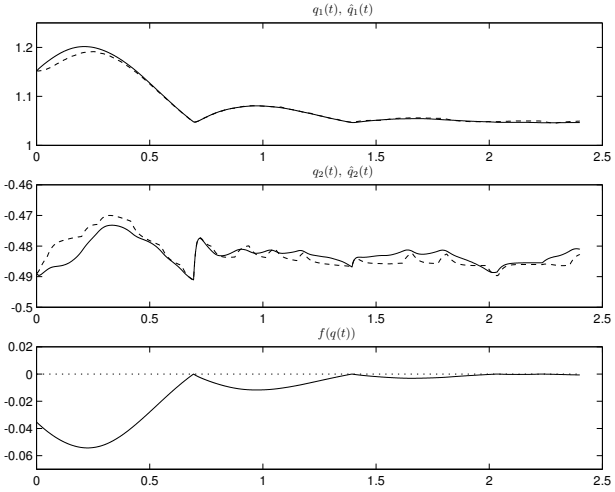

Fig. 12. Time behaviour of the position variables (continuous line) and of their estimates (dashed line) obtained by applying a closed-loop PD control law, making use of the estimates obtained with the full order observer using quantized measurements. In the lowest plot the time behaviour of $f(q(t))$ is reported, together with a dotted line indicating the limit zero value, in order to emphasize the impact times.

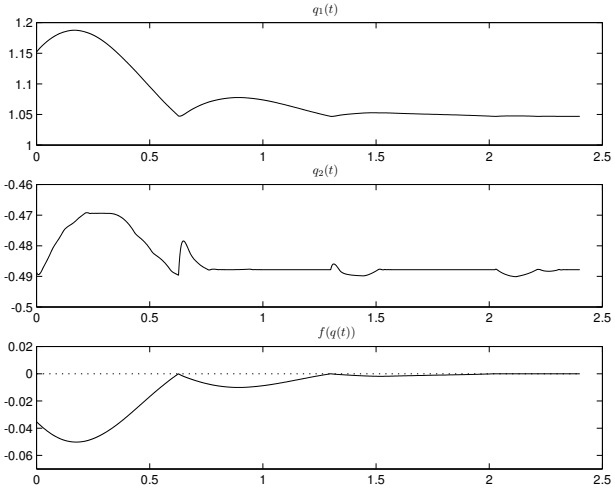

Fig. 13. Time behaviour of the position variables obtained by applying a closed-loop PD control law, making use of the velocity estimates obtained with the reduced order observer using quantized measurements. In the lowest plot the time behaviour of $f(q(t))$ is reported, together with a dotted line indicating the limit zero value, in order to emphasize the impact times.

Acknowledgments

This work has been funded by MURST, ASI and ENEA.

References

[1] B. Brogliato, *Nonsmooth impact mechanics*. Springer Verlag, London, 1996.

[2] L.-B. Wee and M. Walker, "On the dynamics of contact between space robots and configuration control for impact minimization," *IEEE Transactions on Robotics and Automation*, vol. 9, pp. 581 – 591, October 1993.

[3] D. Nenchev and K. Yoshida, "Impact analysis and post-impact motion control issues of a free-floating space robot subject to a force impulse," *IEEE Transactions on Robotics and Automation*, vol. 15, pp. 548 – 557, June 1999.

[4] Y. Shoji, M. Inaba, and T. Fukuda, "Impact control of grasping (robot manipulators)," *IEEE Transactions on Industrial Electronics*, vol. 38, pp. 187 – 194, June 1991.

[5] G. Prokop and F. Pfeiffer, "Synthesis of robot dynamic behavior for environmental interaction," *IEEE Transactions on Robotics and Automation*, vol. 14, pp. 718 – 731, October 1998.

[6] A. Tornambè, "Modelling and controlling one-degree-of-freedom impacts under elastic/plastic deformations," *IEE Proceedings - Control Theory and Applications*, vol. 143, pp. 470 – 476, September 1996.

[7] T.-J. Tarn, Y. Wu, N. Xi, and A. Isidori, "Force regulation and contact transition control," *IEEE Control Systems Magazine*, vol. 16, pp. 32 – 40, February 1996.

[8] M. Indri and A. Tornambè, "Impact model and control of two multi-dof cooperating manipulators," *IEEE Transactions on Automatic Control*, vol. 44, pp. 1297 – 1303, June 1999.

[9] B. Brogliato, S. I. Niculescu, and P. Orhant, "On the control of finite-dimensional mechanical systems with unilateral constraints," *IEEE Transactions on Automatic Control*, vol. 42, no. 2, 1997.

[10] A. Tornambè, "Modeling and control of impact in mechanical systems: theory and experimental results," *IEEE Transactions on Automatic Control*, vol. 44, pp. 294–309, February 1999.

[11] S. Nicosia, P. Tomei, and A. Tornambè, "A nonlinear observer for elastic robots," *IEEE Journal of Robotics and Automation*, vol. 4, no. 1, pp. 45–52, 1998.

[12] S. Nicosia and P. Tomei, "Robot control by using only joint position measurement," *IEEE Transactions on Automatic Control*, vol. 35, pp. 1058–1061, September 1990.

[13] C. Canudas de Wit, N. Fixot, and K. Astrom, "Trajectory tracking in robot manipulators via nonlinear estimated state feedback," *IEEE Journal of Robotics and Automation*, vol. 8, pp. 138–144, February 1992.

[14] H. Berghuis and H. Nijmeijer, "Robust control of robots via linear estimated state feedback," *IEEE Transactions on Automatic Control*, vol. 39, pp. 2159–2162, October 1994.

[15] L. Menini and Antonio Tornambè, "Velocity observers for linear mechanical systems subject to single non-smooth impacts," *Systems & Control Letters*, vol. 43, pp. 193–202, 2001.

[16] Arthur J. Krener and MingQing Xiao. Observers for linearly unobservable nonlinear systems. *Systems and Control Letters*, 46:281–288, 2002.

[17] L. Menini and A. Tornambè, "Velocity observers for non-linear mechanical systems subject to non-smooth impacts," *Automatica*, vol. 38, pp. 2169–2175, December 2002.

[18] S. Galeani and L. Menini and A. Tornambè, "A local observer for linearly observable nonlinear mechanical systems subject to impacts," To appear in *Proceedings of the American Control Conference*, June 2003.